Atmos. Chem. Phys. Discuss., 14, 14439–14470, 2014
www.atmos-chem-phys-discuss.net/14/14439/2014/
doi:10.5194/acpd-14-14439-2014

Atmospheric Chemistry and Physics Discussions

A 2 year record of atmospheric mercury species at a background Southern Hemisphere station on Amsterdam Island

H. Angot[1], M. Barret[1], O. Magand[1], M. Ramonet[2], and A. Dommergue[1]

[1]Univ. Grenoble Alpes/CNRS, Laboratoire de Glaciologie et Géophysique de l'Environnement (LGGE), 38041 Grenoble, France
[2]Laboratoire des Sciences du Climat et de l'Environnement (LSCE/IPSL), CEA-CNRS-UVSQ, Gif-sur-Yvette, Cedex 91191, France

Received: 20 May 2014 – Accepted: 26 May 2014 – Published: 3 June 2014

Correspondence to: H. Angot (helene.angot@lgge.obs.ujf-grenoble.fr)

Published by Copernicus Publications on behalf of the European Geosciences Union.

Abstract

Scarcity of mercury species records in the Southern Hemisphere is a critical weak point for the development of appropriate modeling and regulation scenarios. Under the framework of the "Global Mercury Observation System" (GMOS) project, a monitoring station has been set up on Amsterdam Island (37°48′ S, 77°34′ E) in the remote southern Indian Ocean. For the first time in the Southern Hemisphere, a 2 year record of gaseous elemental mercury (GEM), reactive gaseous mercury (RGM) and particle-bound mercury (PBM) is presented. GEM concentrations were remarkably steady (1.03 ± 0.08 ng m^{-3}) while RGM and PBM concentrations were very low and exhibited a strong variability (mean: 0.34 pg m^{-3} [range: 0.28–4.07 pg m^{-3}] and mean: 0.67 pg m^{-3} [range: 0.28–12.67 pg m^{-3}], respectively). Despite the remoteness of the island, wind sector analysis, air mass back trajectories and the observation of radonic storms highlighted a long-range contribution from the southern African continent to the GEM and PBM budgets in winter during the biomass burning season. Lowest concentrations of GEM were associated with southerly polar and marine air masses from the remote southern Indian Ocean. This unique dataset provides new baseline GEM concentrations in the Southern Hemisphere mid-latitudes for further modeling studies, while mercury speciation along with upcoming wet deposition data will help improving our understanding of mercury cycle in the marine boundary layer.

1 Introduction

Due to its toxicity, persistence, bioaccumulative nature and long-range transport, mercury (Hg) is a global threat to ecosystems and human health. Since the 70's, multiple regulations were implemented to tackle the exposition of populations to this contaminant. In 2013, the United Nations Environment Programme (UNEP) opened for signature a new legally-binding treaty on mercury, giving birth to the Minamata Convention on mercury (UNEP, 2013a). However, research gaps for mercury control policies at

ACPD
14, 14439–14470, 2014

regional or global scale still remain such as our understanding of mercury sources, atmospheric chemistry or deposition processes (Selin et al., 2007).

According to recent estimates (UNEP, 2013b) while 10 % of annual global emissions of atmospheric mercury currently come from natural geological sources – e.g., volcanic emissions, ocean upwelling or mercury-containing rocks –, 30 % are produced by a variety of anthropogenic activities – e.g., coal combustion, cement production, waste incineration or artisanal and small-scale gold mining –, and re-emissions of previously released mercury account for the remaining 60 %. Gaseous elemental mercury (GEM, Hg^0) is the dominant form of atmospheric mercury (Lindberg and Stratton, 1998). It can be oxidized by ozone or free radicals into highly reactive and water-soluble divalent species (Hg^{2+}) and/or particle-bound mercury (PBM) (Lin and Pehkonen, 1999) that can be deposited through wet and dry processes (Lindqvist and Rodhe, 1985).

In remote areas far from any local sources, atmospheric deposition has been recognized as the main source of mercury to the ocean (Lindberg et al., 2007). Mercury can then be reemitted back to the atmosphere via gas exchange (Schroeder and Munthe, 1998) and modeling studies suggest that reemission from oceans is a major contributor to atmospheric concentrations of GEM, particularly in the Southern Hemisphere where oceans were shown to contribute more than half of the surface atmospheric concentration (Strode et al., 2007). Nevertheless, the cycling of mercury at the global scale is not fully understood and the role of oceans still remains unclear, mainly due to a lack of long-term records of atmospheric mercury in the Southern Hemisphere (Pirrone et al., 2013). Although critical to develop comprehensive mercury modeling or regulation scenarios, measurements of mercury species are rarely carried out in remote areas of the Southern Hemisphere. To date observations mainly rely on a few oceanographic campaigns (e.g., Lamborg et al., 1999; Temme et al., 2003a; Witt et al., 2010) and on-going ground-based monitoring surveys at the Cape Point station in South Africa (Slemr et al., 2008) and at Troll, Dumont d'Urville and Concordia stations in Antarctica (Dommergue et al., 2013a, b; Pfaffhuber et al., 2012).

ACPD
14, 14439–14470, 2014

In this context, a monitoring station has been set up on Amsterdam Island, a remote island in the southern Indian Ocean, under the framework of the European Union-financed project "Global Mercury Observation System" (GMOS, http://www.gmos.eu/). The 2 year record of elemental, divalent and particle-bound mercury concentrations presented here is, to the best of the authors' knowledge, the first reported in the Southern Hemisphere mid-latitudes. Along with mercury species, ancillary parameters were analyzed to categorize air masses reaching the station based on their source region. The main objective of this study is to investigate to what extent observations at Amsterdam Island could define Southern Hemisphere mid-latitudes background tropospheric conditions and provide new constraints in multi-scale mercury species cycling models.

2 Materials and methods

2.1 Sampling site description

Amsterdam Island is a small island (55 km^2) located in the southern Indian Ocean (37°48′ S, 77°34′ E), 3400 km and 5000 km upwind from the nearest lands, Madagascar and South Africa, respectively (see Fig. 1). Instrumentation dedicated to the study of atmospheric mercury is located at the Pointe Bénédicte station, at the northwest end of the island, 55 m a.s.l. and 2 km west of the scientific base (30 residents at most). Other monitoring activities are performed at the station for various atmospheric compounds such as ozone (Gros et al., 1998), carbon monoxide (Gros et al., 1999), total aerosol number concentration (Sciare et al., 2001) or carbonaceous aerosols (Sciare et al., 2009).

2.2 Ancillary parameters

Meteorological data – air temperature, relative humidity, barometric pressure, wind speed, and wind direction – were provided by the local meteorological station. Radon 222 and 220 (Rn) are monitored with a precision of 10 % on a 2 h basis. The method is

ACPD
14, 14439–14470, 2014

described in details by Polian et al. (1986) and rely on the measurement over time of the decrease of alpha radioactivity of atmospheric aerosols collected on filters. O_3 measurements have been performed at the Pointe Bénédicte station since 1994, halfway up on a 20 m high tower (Gros et al., 1998). Unfortunately, 2012 and 2013 data are not available due to technical problems.

A new CRDS analyzer was installed at the Pointe Bénédicte station in 2012 for in-situ measurements of CH_4. This instrument (G2301, Picarro) is calibrated once a month with four reference gases (NO11-2004 scale for CH_4).

Air mass back trajectories were calculated using the HYSPLIT (HYbrid Single-Particle Lagrangian Integrated Trajectory) model accessed via NOAA Air Resources Laboratory READY (Real-time Environmental Applications and Display sYstem) website (Draxler and Rolph, 2013; Rolph, 2013). Back trajectories were calculated at 60, 500 and 1000 m a.s.l. – approximate sampling height, upper limit of the marine boundary layer by night, and by day, respectively (Wayne, 1991). Fires counts and chlorophyll *a* data west of Amsterdam Island were obtained via the FIRMS MODIS Fire Archive Download (Davies et al., 2009) and the Giovanni online data system developed and maintained by the NASA GES DISC, respectively.

2.3 Mercury analyzers

Since January 2012 we monitor the 3 most relevant atmospheric mercury species, i.e., GEM, PBM (< 2.5 µm) and reactive gaseous mercury (RGM), the latter consisting in various oxidized gaseous Hg^{2+} compounds and hereafter describing all forms of mercury sampled using a KCl-coated denuder (Landis et al., 2002).

Atmospheric mercury species measurements were performed using a Tekran mercury speciation unit (Tekran 1130 and 1135) coupled to a Tekran 2537B analyzer (Tekran Inc., Toronto, Canada). Concentrations are expressed in ng m^{-3} (GEM) or pg m^{-3} (PBM and RGM), at standard temperature and pressure (273.15 K, 1013.25 hPa). GEM was determined at sub ng m^{-3} levels using a gas-phase mercury analyzer, based on the amalgamation of mercury onto a gold cartridge followed by

ACPD
14, 14439–14470, 2014

a thermal desorption and a detection by an integrated cold vapor atomic fluorescence spectrometer (CVAFS) at 253.7 nm (Bloom and Fitzgerald, 1988; Fitzgerald and Gill, 1979). The presence of two gold cartridges allowed alternating sampling and desorption modes and thus a continuous analysis of GEM in the sample air stream. In order to protect the two gold cartridges against deleterious compounds such as acid gases and halogen compounds, and against particulate matter, the sample air stream was pre-filtered through a sodalime trap and a 0.2 µm PTFE filter.

The speciation unit was located on the roof top of the station, the sampling inlet being at 6 m above the ground, and connected to the 2537B analyzer through a 10 m-long PTFE heated line (50 °C). The sampling resolution was 5 min for GEM and 3 to 4 h for RGM and PBM, with sampling flow rates of 1 L min^{-1} and 10 L min^{-1}, respectively. Measurements were achieved through a multi-step procedure as described elsewhere (Lindberg et al., 2002) using an impactor inlet (2.5 µm cut-off aerodynamic diameter at 10 L min^{-1}), a KCl-coated quartz annular denuder in the 1130 unit, and a quartz regenerable particulate filter (RPF) in the 1135 unit.

2.3.1 Quality assurance and quality control procedures

Fortnightly to monthly routine maintenance operations on the denuder, RPF, sodalime trap and filters, along with thorough cleaning steps and weekly site visits enabled the collection of contamination-free air samples. The accuracy of flow measurements was checked twice a year with a calibrated flow meter (Definer 220). An automatic calibration step of the 2537B analyzer was carried out every 69 h with an internal mercury permeation source. The accuracy of this permeation source was annually checked against manual injections of saturated mercury vapor taken from a temperature controlled vessel, using a Tekran 2505 mercury vapor calibration unit and a Hamilton digital syringe, and following a strict procedure adapted from Dumarey et al. (1985). Both routine and exceptional maintenance were compiled and archived via a software program developed at the LGGE. This software program also enabled a rapid data processing in order to produce clean time-series of GEM, PBM and RGM. Screening criteria for data

ACPD
14, 14439–14470, 2014

validation/invalidation were inspired by standard operative protocols used by GMOS partners (Munthe et al., 2011).

The detection limit for GEM measurements was better than 0.10 ng m^{-3} (Tekran, 2011) and ten injections of 15 µL of saturated mercury vapor were performed to check the repeatability of the system response. The system gave a relative expanded uncertainty of 1 % (95 % confidence level). Validated 5 min GEM data subsets were compiled into hourly-average data when the hourly recovery rate exceeded 50 % (number of valid data records collected vs. that possible over the reporting period).

Whereas there is no robust calibration technique of the Tekran speciation unit and no certified reference material available, the precision of RGM and PBM measurements was shown to be of 15 % (Landis et al., 2002). The sampling resolution was shifted from 3 to 4 h after a few days due to very low RGM and PBM concentrations, and the detection limit therefore decreased from better than 0.42 pg m^{-3} to better than 0.28 pg m^{-3} based on the sampling volumes and GEM detection limit (Wang et al., 2014). Only 15 % and 50 % of RGM and PBM measurements, respectively, were above the estimated limits of detection. Values 3.3 times above the stated detection limits, i.e. reliably quantified, will be discussed thereafter and referred to as RGM and PBM events. However, below-detection limit values will not be discarded when calculating the mean of the distributions, but will be replaced by a fixed non-variable value equal to the limit of detection.

Several studies (Gustin et al., 2013; Huang et al., 2013) highlighted the inefficient collection of gaseous oxidized mercury compounds with a KCl-coated denuder in the Tekran technique, leading to an underestimation of reactive mercury concentrations. As suggested by Wang et al. (2014), RGM data reported in this study should thus only be compared with the existing Tekran-based literature.

ACPD
14, 14439–14470, 2014

3 Results and discussion

3.1 Meteorological data

Climate is mild oceanic, with frequent presence of clouds. Seasonal boundaries were defined as follows: winter from July to September and summer from December to February, in line with other studies performed at Amsterdam Island (Gros et al., 1998; Nguyen et al., 1990; Sciare et al., 2009). During the two-year period under discussion here (January 2012 till December 2013), the monthly median air temperature ranged from 11 °C in austral winter to 17 °C in austral summer, while the monthly median relative humidity remained high and ranged from 65 to 85 % most of the year. Precipitations were very frequent with total precipitations of 1262 mm in 2012 and 1128 mm in 2013, in good agreement with the 1124 mm 40 year average reported by Miller et al. (1993). Wind speed remained comparatively high throughout the year (from 5 to 15 $m\,s^{-1}$); strong northwesterly winds peaking during winter months when the roaring forties are at a maximum (see Fig. 2).

3.2 Gaseous elemental mercury concentrations

3.2.1 Seasonality and contribution from biomass burning

GEM concentrations were very steady with an average hourly mean concentration of $1.03 \pm 0.08\,ng\,m^{-3}$ (mean ± standard deviation, range: 0.72–1.55 $ng\,m^{-3}$; $n = 10285$, see Fig. 3). GEM data are lower than concentrations reported in the Northern Hemisphere (e.g., Laurier et al., 2003) but well within the expected range for a remote marine site in the Southern Hemisphere. Indeed, Witt et al. (2010) measured a mean TGM (Total Gaseous Mercury defined as the sum of gaseous mercury species) concentration of $1.24 \pm 0.06\,ng\,m^{-3}$ in the Indian Ocean at latitudes ranging from 9 to 21° S, while TGM concentrations ranged from 1.20 to 1.40 $ng\,m^{-3}$ at the Cape Point station, South Africa (34°21′ S, 18°29′ E) between 1995 and 2004 (Slemr et al., 2008) and GEM

ACPD
14, 14439–14470, 2014

concentrations amounted to $0.93 \pm 0.19\,ng\,m^{-3}$ at Troll station in Antarctica (Pfaffhuber et al., 2012). GEM concentrations measured at Amsterdam Island are furthermore highly consistent with data reported by Wang et al. (2014) in the marine boundary layer over the equator at Galápagos Islands (0°57′ S, 90°58′ W; $1.08 \pm 0.17\,ng\,m^{-3}$) despite occasional influence of northern hemispheric air at this station. A comprehensive comparison of mercury concentrations measured in the Southern Hemisphere is given in Slemr et al. (2014).

Whereas TGM and GEM concentrations at the Cape Point station and at Galápagos Islands, respectively, showed a seasonal variation (Slemr et al., 2008; Wang et al., 2014), with minimum in winter and maximum in summer, GEM data at Amsterdam Island did follow an opposite trend, with slightly but significantly higher concentrations in winter than in summer ($1.06 \pm 0.09\,ng\,m^{-3}$ vs. $1.04 \pm 0.07\,ng\,m^{-3}$, p value $< 2.2 \times 10^{-16}$, Mann–Whitney test, see Fig. 4a).

This seasonality of GEM concentrations is in agreement with more frequent air masses originating from southern Africa (northwesterly winds) in winter. In order to further test this hypothesis GEM data were sorted according to wind direction imposing a strict criterion on wind speed ($> 8\,m\,s^{-1}$) to remove any local influence (Monfray et al., 1987). With north at 0°, southerly (S) winds ranged from 100 to 250° and northwesterly (NW) winds from 250 to 300°. GEM concentrations monitored during periods of NW flow where shown to be significantly higher than during S flow ($1.05 \pm 0.08\,ng\,m^{-3}$ ($n = 2833$) vs. $1.01 \pm 0.08\,ng\,m^{-3}$ ($n = 822$), p value $< 2.2 \times 10^{-16}$, Mann–Whitney test, see Fig. 4b).

The GEM budget on the island could be enhanced during winter months by long-range transport during the burning season in southern Africa. 2012 and 2013 satellite observations of fires west of Amsterdam Island (latitude ranging from 3 to 53° S and longitude from 10 to 73° E) showed that the burning season extended from May to October, peaking between June and September (see Fig. 5), in line with observations reported by Cooke et al. (1996). This assumption is also supported by the concomitant seasonal maxima on Amsterdam Island of equivalent black carbon, non-sea-salt

ACPD
14, 14439–14470, 2014

potassium and oxalate, two compounds commonly used as tracers for biomass burning (Sciare et al., 2009), and CO (Gros et al., 1999).

3.2.2 Short-time variations

The atmosphere at Amsterdam Island could define background tropospheric conditions, with minimum perturbation from anthropogenic influences. However, as reported by Balkanski and Jacob (1990), the rapid export of air from southern Africa to the subantarctic Indian Ocean could constitute a major source of pollution to southern mid-latitudes.

The background variability of GEM concentrations was assessed following a procedure adapted from Gros et al. (1999) calculating the difference, dGEM, between hourly GEM concentrations and the monthly mean. dGEM events higher than $\pm 0.18\,\mathrm{ng\,m^{-3}}$, 3 times the mean monthly standard deviation of dGEM measurements, were further investigated.

^{222}Rn, decay product of ^{238}U with a 3.8 day half-life, is particularly well suited as a tracer of continental air over the oceans (Balkanski and Jacob, 1990). On the other hand, ^{220}Rn and its daughter ^{212}Pb, due to 54 s and 10.6 h half-lives, respectively, can only be attributed to local outgassing from Amsterdam Island's soil and not to any marine nor remote continental source (Polian et al., 1986). Therefore, ^{222}Rn activities below $100\,\mathrm{mBq\,m^{-3}}$ are considered as typical for marine air (Brunke et al., 2004), whereas air with ^{222}Rn activity above $100\,\mathrm{mBq\,m^{-3}}$ along with a ^{220}Rn (^{212}Pb) activity of a few $\mathrm{mBq\,m^{-3}}$ only is considered to be significantly influenced by a remote continent (Gros et al., 1999). Rapid and sharp variations of ^{222}Rn activity, referred to as "radonic storms" (Lambert et al., 1970), could be observed at Amsterdam Island, usually peaking around $400\,\mathrm{mBq\,m^{-3}}$, and exceptionally reaching $1000\,\mathrm{mBq\,m^{-3}}$.

The local production of radon on Amsterdam Island can explain some radonic storms such as the one observed on 13 December 2012 (see Fig. 6a). As reported by Polian et al. (1986), they are associated with low wind speeds (below $5\,\mathrm{m\,s^{-1}}$) and meteorological conditions corresponding to a low atmospheric eddy diffusion. The back

ACPD
14, 14439–14470, 2014

trajectories ending on 13 December 2012 on Amsterdam Island (see Fig. 7a) meander over the ocean, and low south-eastern/eastern winds prevailed ahead of ^{222}Rn and ^{220}Rn peaks, in good agreement with an influence from the island and local radon exhausts. The associated high GEM event (dGEM > 0.18 ng m^{-3}; see Fig. 6b) was significantly positively correlated with ^{222}Rn and ^{220}Rn activities (r = 0.83, p value = 0.005 and r = 0.80, p value = 0.010 respectively, Spearman test) and can therefore be attributed to a local non-anthropogenic source as no noteworthy activity occurred at the sampling station nor on the scientific base.

On the contrary, most of sharp high GEM events (dGEM > 0.18 ng m^{-3}) were associated with ^{222}Rn peaks, strong winds and ^{220}Rn activities of a few mBq m^{-3} only, and therefore ascribed to continental air mass advection. For example, the high GEM event occurring on 21 September 2013 (see Fig. 6d) was associated with a ^{222}Rn peak of about 200 mBq m^{-3}, a low ^{220}Rn activity and 15 m s^{-1} winds (see Fig. 6c). This high GEM event was significantly positively correlated with ^{222}Rn activities (r = 0.79, p value = 8.5 × 10^{-5}, Spearman test). The back trajectories ending on 21 September 2013 on Amsterdam Island (see Fig. 7c) pass near the southern African continent and Madagascar, confirming the continental origin of the air at the time of enhanced ^{222}Rn activity and GEM concentrations. Although back trajectories indicate no direct passage over the continent, a continental origin of the air is not unlikely since that range of ^{222}Rn activities has already been measured for trajectories calculated to have passed more than 100 km away from mainland Australia (Whittlestone et al., 1998).

As for high GEM events, continental induced radonic storms mainly occurred between June and October reflecting the seasonality of wind direction at Amsterdam Island and of long-range transport from the southern African continent.

As illustrated on Figs. 6d, 7b and d, low GEM events (dGEM < 0.18 ng m^{-3}) were well correlated with trajectories passing over Antarctica. This continent being almost all ice-covered, local emission of ^{222}Rn and ^{220}Rn is low (Polian et al., 1986) explaining why low GEM events are not associated with any ^{222}Rn peak.

ACPD
14, 14439–14470, 2014

These short-term variations suggest that cleaner air masses originate from the remote southern Indian Ocean while NW air masses are influenced by continental southern Africa, as previously assumed by several authors (Gros et al., 1999; Miller et al., 1993; Williams et al., 2001).

3.2.3 Southern Hemisphere mid-latitudes baseline concentrations for modeling studies

Over the 2 years, high and low GEM events observed did not significantly affect the overall mean. Indeed, the mean and the median are equal. Medians have been calculated for each month and differ in average from the arithmetical means by 0.90 % which is less than the relative expanded uncertainty of the system response. GEM concentrations at Amsterdam Island can be considered as baseline concentrations and be used as is in modeling studies. However, a slight but significant seasonal cycle was highlighted and despite the remoteness of the station an influence of biomass burning was observed in winter. Biomass burning affects all the mid-latitude belt of the Southern Hemisphere at least and can be considered as a widespread pollution (Fishman et al., 1991; Gros et al., 1999). Biomass burning slightly contributes to the background GEM level in this region and should be carefully considered in modeling studies when dealing with seasonality of GEM concentrations in the Southern Hemisphere mid-latitudes.

3.3 Oxidized mercury species: seasonality and sources

A 2 year record of RGM and PBM concentrations is presented hereafter – the longest ever reported in the Southern Hemisphere. Concentrations at Amsterdam Island were very low – at the lower end of the range reported during oceanographic campaigns (Laurier and Mason, 2007; Laurier et al., 2003; Temme et al., 2003b), and exhibited a strong variability (see Fig. 3). RGM and PBM mean concentrations amounted to 0.34 pg m^{-3} [range: 0.28–4.07 pg m^{-3}] and 0.67 pg m^{-3} [range: 0.28–12.67 pg m^{-3}], respectively. Such low RGM and PBM concentrations at Amsterdam Island could be

ACPD
14, 14439–14470, 2014

explained by the very frequent drizzle efficiently scavenging oxidized mercury species. To further investigate this assumption, a precipitation collector was set up on the island at the beginning of 2013 in order to analyze mercury species in rainwater.

3.3.1 Reactive gaseous mercury

RGM can be primary emitted from point sources or originate from an oxidation of GEM. Due to a short lifetime RGM can only be transported tens to hundreds of kilometers (Schroeder and Munthe, 1998). Monitoring of primary emitted RGM at Amsterdam Island is therefore unlikely.

RGM in the marine boundary layer has been reported to originate from: (i) a photochemically driven oxidation of GEM (e.g., Laurier et al., 2003), (ii) an UV-correlated evasional flux of dissolved gaseous mercury from surface water (e.g., Laurier et al., 2003), or (iii) through entrainment from the free troposphere (Holmes et al., 2009).

Oxidation pathways of GEM involving ozone (O_3), the hydroxyl radical (OH), atomic bromine (Br) or nitrogen dioxide (NO_2), or a combination of them, have been suggested by modeling and field studies (e.g., Wang et al., 2014). Our understanding of RGM production mechanisms at Amsterdam Island is still limited and no anti-correlation between RGM and GEM concentrations, suggesting an in-situ GEM oxidation, was found. Further field studies to better understand the major oxidation pathways at stake would require a lower detection limit for RGM, an operative monitoring of ozone, and simultaneous measurements of other trace gases such as halogen oxides (BrO and IO) and nitrogen dioxide.

A slight but significant seasonal trend in RGM concentrations was highlighted (1.34 ± 0.45 pg m^{-3} in winter vs. 1.58 ± 0.35 pg m^{-3} in summer, p value = 0.01, Mann–Whitney test), and RGM events occurred about 55 % of the time between December and March, i.e. in summer (see Fig. 8), in line with an enhanced photochemistry in summer. While a significant negative correlation between CH_4 and air temperature was observed ($r = -0.638$, $p < 2.2 \times 10^{-16}$, Spearman test), consistent with its photochemical destruction by the hydroxyl radical (Khalil and Rasmussen, 1983), no correlation was

ACPD
14, 14439–14470, 2014

found between RGM concentrations and air temperature, or any other meteorological parameter.

Marine organic aerosol concentrations at Amsterdam Island have been shown to be directly related to the seasonal cycle of chlorophyll *a* (Sciare et al., 2009) and dimethylsulfide (DMS) concentrations peaking in summer have been reported on the island, in line with an enhanced biological activity (Nguyen et al., 1990; Sciare et al., 1999). The production of halogen species, photolytically leading to atomic bromine, could be driven by biological activity (Gschwend et al., 1985). Unlike the oceanic region surrounding Amsterdam Island, an area located in a southwest upwind sector covering the subtropical front (see Fig. 9) is highly productive, with a marine productivity (characterized by chlorophyll *a* concentration) peaking from December to January and sometimes in late summer (March–April) (Sciare et al., 2009), in agreement with peaks of RGM events.

3.3.2 Particle-bound mercury

PBM originates from the adsorption of GEM or oxidized mercury species onto particles. It can be primary emitted from point sources or form in the atmosphere. Field and modeling studies (e.g., Steffen et al., 2014) suggested that the partitioning of mercury onto particles might be driven by air temperature and aerosol particle loadings.

PBM concentrations at Amsterdam Island followed a seasonal trend with significantly higher concentrations in winter than in summer ($2.18 \pm 1.56\,\mathrm{ng\,m^{-3}}$ vs. $1.79 \pm 1.15\,\mathrm{pg\,m^{-3}}$, p value = 0.027, Mann–Whitney test). Higher PBM concentrations were recorded during the strongest NW winds episodes (see Fig. 10), suggesting an enhanced long-range transport of PBM from continental southern Africa during strong NW winds episodes. The higher number of PBM events in 2013 (see Fig. 8) is in good agreement with about twice as many continental induced radonic storms observed at Amsterdam Island in 2013 than in 2012.

PBM events occurred about 55 % of the time between August and October in 2012 and 2013 (see Fig. 8) and were significantly positively correlated with fires counts west of Amsterdam Island (r = 0.56, p value = 0.005, Spearman test). This result is

ACPD
14, 14439–14470, 2014

consistent with other observations of enhanced PBM concentrations during wildfires (Finley et al., 2009). However, peaks of biomass fires counts and PBM events did not coincide in time; the maxima being observed for June–September and August–October, respectively. The seasonality of aerosol optical depth (AOD) in the Southern Hemisphere Africa biomass burning region was extensively monitored by the Cimel sun-sky radiometer at the AERONET site in Mongu, Zambia. 1995 to 2009 measurements highlighted that the monthly means of Level 2 direct sun-measured 500 nm AOD at Mongu reached a peak from August to October (Eck et al., 2013), in line with the PBM events peak observed at Amsterdam Island. This time lag between seasonal peaks in fire counts and emissions has already been pointed out by Swap et al. (2003), but its origin remains unclear. It has been attributed either to unusual synoptic conditions favoring eastward transport of pollution over measurement sites (Stein et al., 2003; Swap et al., 2003) or to undetected/highly emissive denser wooded vegetation burns at the end of the fire season (Edwards et al., 2006).

4 Conclusion

Wind sector analysis, air mass back trajectories and the observation of radonic storms led to the important conclusion that despite the remoteness of Amsterdam Island the rapid export of air from the southern African continent during the biomass burning season (winter) contributes to GEM and PBM budgets on the island. Lowest GEM concentrations are associated with southerly polar and marine air masses from the remote southern Indian Ocean. This dataset provides a new insight into baseline concentrations of mercury species in the Southern Hemisphere mid-latitudes and opens the way for new avenues in future modeling studies. Our understanding of mercury cycle in the marine boundary layer over Amsterdam Island is still limited. It represents a real challenge given harsh weather conditions – with a very frequent drizzle most certainly scavenging oxidized species –, and technical and logistical limitations. Further studies involving wet deposition, a lower detection limit for oxidized species, and simultaneous

ACPD
14, 14439–14470, 2014

measurements of other trace gases would be welcome to improve our understanding of oxidation mechanisms and deposition processes.

Acknowledgements. This work contributes to the EU-FP7 project Global Mercury Observation System (GMOS). Logistical and financial support was provided by the French Polar Institute IPEV (Program 1028, GMOStral). Financial support was also provided by a grant from Labex OSUG@2020 (ANR10 LABX56) and LEFE CNRS/INSU (program SAMOA). We deeply thank the overwintering staff: B. Brouillard, J. Chastain, E. Coz, A. Croguennoc, M. Le Dréau and V. Lucaire, and AD acknowledges the Institut Universitaire de France. We also gratefully acknowledge the MODIS mission scientists and associated NASA personnel for the production of the data used in this research effort, and the NOAA Air Resources Laboratory (ARL) for the provision of the READY website (http://www.ready.noaa.gov) used in this publication.

References

Balkanski, Y. J. and Jacob, D. J.: Transport of continental air to the subantarctic Indian Ocean, Tellus B, 42, 62–75, 1990.

Bloom, N. S. and Fitzgerald, W. F.: Determination of volatile mercury species at the picogram level by low temperature gas chromatography with cold-vapor atomic fluorescence detection, Anal. Chim. Acta, 208, 151–161, 1988.

Brunke, E.-G., Labuschagne, C., Parker, B., Scheel, H. E., and Whittlestone, S.: Baseline air mass selection at Cape Point, South Africa: application of ^{222}Rn and other filter criteria to CO_2, Atmos. Environ., 38, 5693–5702, 2004.

Cooke, W. F., Koffi, B., and Grégoire, J.-M.: Seasonality of vegetation fires in Africa from remote sensing data and application to a global chemistry model, J. Geophys. Res., 101, 21051–21065, 1996.

Davies, D. K., Ilavajhala, S., Wong, M. M., and Justice, C. O.: Fire information for resource management system: archiving and distributing MODIS active fire data, IEEE T. Geosci. Remote, 47, 72–79, 2009.

Dommergue, A., Ferrari, C. P., Magand, O., Barret, M., Gratz, L. E., Pirrone, N., and Sprovieri, F.: Monitoring of gaseous elemental mercury in central Antarctica at Dome Concordia, in: Proceedings of the 16th International Conference on Heavy Metals in the Environment, E3S Web of Conferences, Rome, Italy, 23–27 September 2012, 27005, 2013.

ACPD
14, 14439–14470, 2014

Dommergue, A., Vogel, N., Ferrari, C. P., Magand, O., and Barret, M.: Preliminary results from a continuous record of atmospheric gaseous mercury at the coastal station Dumont d'Urville in Antarctica, in: Proceedings of the 16th International Conference on Heavy Metals in the Environment, E3S Web of Conferences, Rome, Italy, 23–27 September 2012, 27005, 2013.

Draxler, R. R. and Rolph, G. D.: HYSPLIT (HYbrid Single-Particle Lagrangian Integrated Trajectory) Model access via NOAA ARL READY Website, available at: http://www.arl.noaa.gov/HYSPLIT.php (last access: 24 February 2014), NOAA Air Resources Laboratory, College Park, MD, 2013.

Dumarey, R., Temmerman, E., Dams, R., and Hoste, J.: The accuracy of the vapour injection calibration method for the determination of mercury by amalgamation/cold vapour atomic spectrometry, Anal. Chim. Acta, 170, 337–340, 1985.

Eck, T. F., Holben, B. N., Reid, J. S., Mukelabai, M. M., Piketh, S. J., Torres, O., Jethva, H. T., Hyer, E. J., Ward, D. E., Dubovik, O., Sinyuk, A., Schafer, J. S., Giles, D. M., Sorokin, M., Smirnov, A., and Slutsker, I.: A seasonal trend of single scattering albedo in southern African biomass-burning particles: implications for satellite products biomass-burning sources, J. Geophys. Res., 118, 6414–6432, 2013.

Edwards, D. P., Emmons, L. K., Gille, J. C., Chu, A., Attié, J.-L., Giglio, L., Wood, S. W., Haywood, J., Deeter, M. N., Massie, S. T., Ziskin, D. C., and Drummond, J. R.: Satellite-observed pollution from Southern Hemisphere biomass burning, J. Geophys. Res., 111, D14312, 1–17, 2006.

Finley, B. D., Swartzendruber, P. C., and Jaffe, D. A.: Particulate mercury emissions in regional wildfire plumes observed at the mount bachelor observatory, Atmos. Environ., 43, 6074–6083, 2009.

Fishman, J., Fakhruzzaman, K., Cros, B., and Nganga, D.: Identification of widespread pollution in the Southern Hemisphere deduced from satellite analyses, Science, 252, 1693–1696, 1991.

Fitzgerald, W. F. and Gill, G. A.: Subnanogram determination of mercury by two-stage gold amalgamation and gas detection applied to atmospheric analysis, Anal. Chem., 51, 1714–1720, 1979.

Gros, V., Poisson, N., Martin, D., Kanakidou, M., and Bonsang, B.: Observations and modeling of the seasonal variation of surface ozone at Amsterdam Island: 1994–1996, J. Geophys. Res., 103, no. D21, 28.103–109, 1998.

ACPD
14, 14439–14470, 2014

Gros, V., Bonsang, B., Martin, D., and Novelli, P. C.: Carbon monoxide short term measurements at Amsterdam Island: estimation of biomass burning rates, Chemosphere Global Change Sci., 1, 163–172, 1999.
Gschwend, P. M., MacFarlane, J. K., and Newman, K. A.: Volatile halogenated organic compounds released to seawater from temperate marine macroalgae, Science, 227, 1033–1035, 1985.
Gustin, M. S., Huang, J., Miller, M. B., Peterson, C., Jaffe, D. A., Ambrose, J., Finley, B. D., Lyman, S. N., Call, K., Talbot, R., Feddersen, D., Mao, H., and Lindberg, S. E.: Do we understand what the mercury speciation instruments are actually measuring? Results of RAMIX, Environ. Sci. Technol., 47, 7295–7306, 2013.
Holmes, C. D., Jacob, D. J., Mason, R. P., and Jaffe, D. A.: Sources and deposition of reactive gaseous mercury in the marine atmosphere, Atmos. Environ., 43, 2278–2285, 2009.
Huang, J., Miller, M. B., Weiss-Penzias, P., and Gustin, M. S.: Comparison of gaseous oxidized mercury measured by KCl-coated denuders, and nylon and cation exchange membranes, Environ. Sci. Technol., 47, 7307–7316, 2013.
Khalil, M. A. K. and Rasmussen, R. A.: Sources, sinks, and seasonal cycles of atmospheric methane, J. Geophys. Res., 88, 5131–5144, 1983.
Lambert, G., Polian, G., and Taupin, D.: Existence of periodicity in radon concentrations and in the large-scale circulation at latitudes between 40° and 70° south, J. Geophys. Res., 75, 2341–2345, 1970.
Lamborg, C. H., Rolfhus, K. R., Fitzgerald, W. F., and Kim, G.: The atmospheric cycling and air–sea exchange of mercury species in the south and equatorial atlantic ocean, Deep-Sea Res. Pt. II, 46, 957–977, 1999.
Landis, M. S., Stevens, R. K., Schaedlich, F., and Prestbo, E. M.: Development and characterization of an annular denuder methodology for the measurement of divalent inorganic reactive gaseous mercury in ambient air, Environ. Sci. Technol., 36, 3000–3009, 2002.
Laurier, F. and Mason, R. P.: Mercury concentration and speciation in the coastal and open ocean boundary layer, J. Geophys. Res., 112, D06302, doi:10.1029/2006JD007320, 2007.
Laurier, F., Mason, R. P., Whalin, L., and Kato, S.: Reactive gaseous mercury formation in the north pacific ocean's marine boundary layer: a potential role of halogen chemistry, J. Geophys. Res., 108, 4529, doi:10.1029/2003JD003625, 2003.
Lin, C.-J. and Pehkonen, S. O.: The chemistry of atmospheric mercury: a review, Atmos. Environ., 33, 2067–2079, 1999.

ACPD
14, 14439–14470, 2014

Lindberg, S. E. and Stratton, W. J.: Atmospheric mercury speciation: concentrations and behavior of reactive gaseous mercury in ambient air, Environ. Sci. Technol., 32, 49–57, 1998.
Lindberg, S. E., Brooks, S., Lin, C.-J., Scott, K. J., Landis, M. S., Stevens, R. K., Goodsite, M. E., and Richter, A.: Dynamic oxidation of gaseous mercury in the arctic troposphere at polar sunrise, Environ. Sci. Technol., 36, 1245–1256, 2002.
Lindberg, S. E., Bullock, R., Ebinghaus, R., Engstrom, D., Feng, X., Fitzgerald, W. F., Pirrone, N., Prestbo, E., and Seigneur, C.: A synthesis of progress and uncertainties in attributing the sources of mercury in deposition, Ambio, 36, 19–32, 2007.
Lindqvist, O. and Rodhe, H.: Atmospheric mercury – a review, Tellus B, 37, 136–159, 1985.
Miller, J. M., Moody, J. L., Harris, J. M., and Gaudry, A.: A 10-year trajectory flow climatology for Amsterdam island, 1980–1989, Atmos. Environ., 27, 1909–1916, 1993.
Monfray, P., Gaudry, A., Polian, G., and Lambert, G.: Seasonal variations of atmospheric CO_2 in the southern Indian Ocean, Tellus B, 39, 67–71, 1987.
Munthe, J., Sprovieri, F., Horvat, M., and Ebinghaus, R.: SOPs and QA/QC protocols regarding measurements of TGM, GEM, RGM, TPM and mercury in precipitation in cooperation with WP3, WP4 and WP5, GMOS deliverable 6.1, CNR-IIA, IVL, available at: http://www.gmos.eu (last access: 3 March 2014), 2011.
Nguyen, B. C., Mihalopoulos, N., and Belviso, S.: Seasonal variation of atmospheric dimethylsulfide at Amsterdam Island in the southern Indian Ocean, J. Atmos. Chem., 11, 123–141, 1990.
Pfaffhuber, K. A., Berg, T., Hirdman, D., and Stohl, A.: Atmospheric mercury observations from Antarctica: seasonal variation and source and sink region calculations, Atmos. Chem. Phys., 12, 3241–3251, doi:10.5194/acp-12-3241-2012, 2012.
Pirrone, N., Aas, W., Cinnirella, S., Ebinghaus, R., Hedgecock, I. M., Pacyna, J. M., Sprovieri, F., and Sunderland, E. M.: Toward the next generation of air quality monitoring: mercury, Atmos. Environ., 80, 599–611, 2013.
Polian, G., Lambert, G., Ardouin, B., and Jegou, A.: Long range transport of continental radon in subantarctic and antarctic areas, Tellus B, 38, 178–189, 1986.
Rolph, G. D.: Real-time Environmental Applications and Display sYstem (READY) Website, available at: http://www.ready.noaa.gov (last access: 24 February 2014), NOAA Air Resources Laboratory, College Park, MD, 2013.
Schroeder, W. H. and Munthe, J.: Atmospheric mercury – an overview, Atmos. Environ., 32, 809–822, 1998.

ACPD
14, 14439–14470, 2014

Sciare, J., Mihalopoulos, N., and Nguyen, B. C.: Summertime seawater concentrations of dimethylsulfide in the western Indian Ocean: reconciliation of fluxes and spatial variability with long-term atmospheric observations, J. Atmos. Chem., 32, 357–373, 1999.

Sciare, J., Mihalopoulos, N., and Baboukas, E.: Short-term variations of dimethylsulfide and its oxidation products at Amsterdam Island during summer time, J. Atmos. Chem., 39, 281–302, 2001.

Sciare, J., Favez, O., Sarda-Estève, R., Oikonomou, K., Cachier, H., and Kazan, V.: Long-term observations of carbonaceous aerosols in the austral ocean atmosphere: evidence of a biogenic marine organic source, J. Geophys. Res., 114, D15302, doi:10.1029/2009JD011998, 2009.

Selin, N. E., Jacob, D. J., Park, R. J., Yantosca, R. M., Strode, S., Jaeglé, L., and Jaffe, D. A.: Chemical cycling and deposition of atmospheric mercury: global constraints from observations, J. Geophys. Res., 112, D02308, doi:10.1029/2006JD007450, 2007.

Slemr, F., Brunke, E.-G., Labuschagne, C., and Ebinghaus, R.: Total gaseous mercury concentrations at the Cape Point GAW station and their seasonality, Geophys. Res. Lett., 35, L11807, doi:10.1029/2008GL033741, 2008.

Slemr, F., Angot, H., Dommergue, A., Barret, M., Magand, O., Weigelt, A., Ebinghaus, R., Brunke, E.-G., and Pfaffhuber, K. A.: Comparison of mercury concentrations measured at several sites in Southern Hemisphere, in preparation, 2014.

Steffen, A., Bottenheim, J., Cole, A., Ebinghaus, R., Lawson, G., and Leaitch, W. R.: Atmospheric mercury speciation and mercury in snow over time at Alert, Canada, Atmos. Chem. Phys., 14, 2219–2231, doi:10.5194/acp-14-2219-2014, 2014.

Stein, D. C., Swap, R. J., Greco, S., Piketh, S. J., Macko, S. A., Doddridge, B. G., Elias, T., and Bruintjes, R. T.: Haze layer characterization and associated meteorological controls along the eastern coastal region of southern africa, J. Geophys. Res., 108, 8506, doi:10.1029/2002JD003237 2003.

Strode, S. A., Jaeglé, L., Selin, N. E., Jacob, D. J., Park, R. J., Yantosca, R. M., Mason, R. P., and Slemr, F.: Air–sea exchange in the glocal mercury cycle, Global Biogeochem. Cy., 21, GB1017, doi:10.1029/2006GB002766, 2007.

Swap, R. J., Annegarn, H. J., Suttles, J. T., King, M. D., Platnick, S., Privette, J. L., and Scholes, R. J.: Africa burning: a thematic analysis of the southern african regional science initiative (SAFARI 2000), J. Geophys. Res., 108, 8465, doi:10.1029/2003JD003747, 2003.

ACPD
14, 14439–14470, 2014

Tekran: Tekran 2537 Mercury Monitor Detection Limit, Summary of Known Estimates, Tekran Instruments Corp., Toronto, ON, Canada, 2011.
Temme, C., Slemr, F., Ebinghaus, R., and Einax, J. W.: Distribution of mercury over the atlantic ocean in 1996 and 1999–2001, Atmos. Environ., 37, 1889–1897, 2003a.
Temme, C., Einax, J. W., Ebinghaus, R., and Schroeder, W. H.: Measurements of atmospheric mercury species at a coastal site in the antarctic and over the atlantic ocean during polar summer, Environ. Sci. Technol., 37, 22–31, 2003b.
UNEP: Text of the Minamata Convention on Mercury for adoption by the Conference of Plenipotentiaries, unep.org, 31 July, available at: http://www.unep.org/hazardoussubstances/Portals/9/Mercury/Documents/dipcon/CONF_3_MinamataConventiononMercury_final2608_e.pdf (last access: 28 February 2014), 2013a.
UNEP: Global Mercury Assessment 2013: Sources, Emissions, Releases and Environmental Transport, UNEP Chemicals Branch, Geneva, Switzerland, 44 pp., 2013b.
Wang, F., Saiz-Lopez, A., Mahajan, A. S., Gómez Martín, J. C., Armstrong, D., Lemes, M., Hay, T., and Prados-Roman, C.: Enhanced production of oxidised mercury over the tropical Pacific Ocean: a key missing oxidation pathway, Atmos. Chem. Phys., 14, 1323–1335, doi:10.5194/acp-14-1323-2014, 2014.
Wayne, R. P.: Chemistry of Atmospheres, 2nd edn., Oxford University Press, Oxford, 1991.
Whittlestone, S., Gras, J. L., and Siems, S. T.: Surface air mass origins during the first aerosol characterization experiment (ACE 1), J. Geophys. Res., 103, 16341–16350, 1998.
Williams, J., Gros, V., Bonsang, B., and Kazan, V.: HO cycle in 1997 and 1998 over the southern Indian Ocean derived from CO, radon, and hydrocarbon measurements made at Amsterdam island, J. Geophys. Res., 106, 12719–12725, doi:10.1029/2001JD900116, 2001.
Witt, M. L. I., Mather, T. A., Baker, A. R., De Hoog, J. C. M., and Pyle, D. M.: Atmospheric trace metals over the south-west Indian Ocean: total gaseous mercury, aerosol trace metal concentrations and lead isotope ratios, Mar. Chem., 121, 2–16, 2010.

ACPD
14, 14439–14470, 2014

Figure 1. Location of Amsterdam Island (AMS), Cape Point (CPT), Troll (TRL), Dumont d'Urville (DDU), and Concordia (DMC) stations – projection centered over Amsterdam Island.

ACPD
14, 14439–14470, 2014

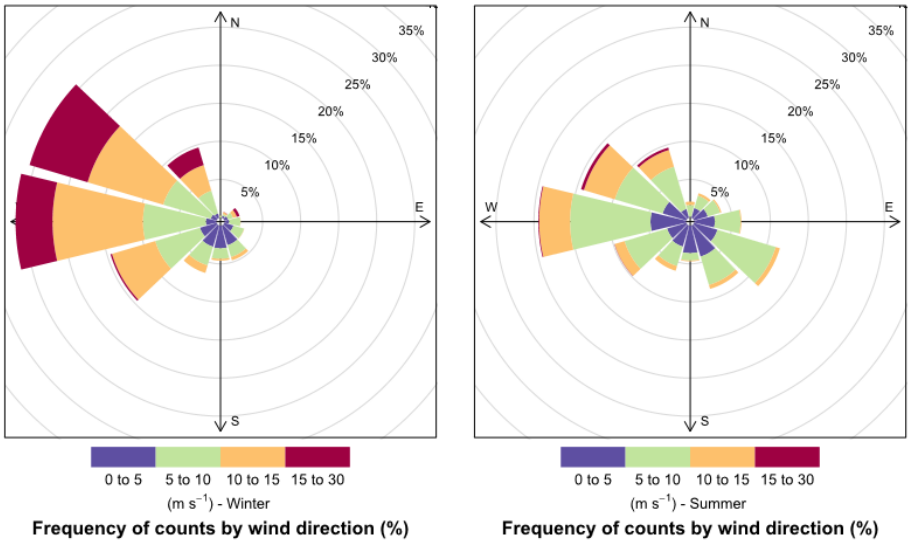

Figure 2. Wind direction and wind speed ($m\,s^{-1}$) in winter (July to September) and summer (December to February) at the Pointe Bénédicte station. N: North, E: East, S: South, W: West.

ACPD
14, 14439–14470, 2014

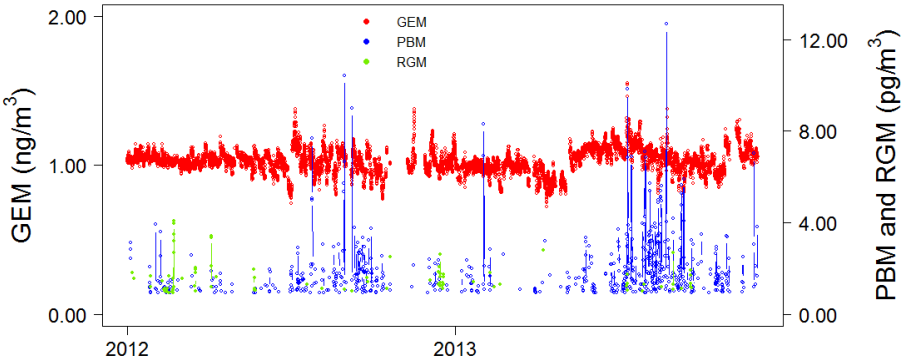

Figure 3. Hourly-average gaseous elemental mercury (GEM, red) concentrations (ng m^{-3}), particle-bound mercury (PBM, blue) and reactive gaseous mercury (RGM, green) concentrations (pg m^{-3}) measured at Amsterdam Island from January 2012 to December 2013.

ACPD
14, 14439–14470, 2014

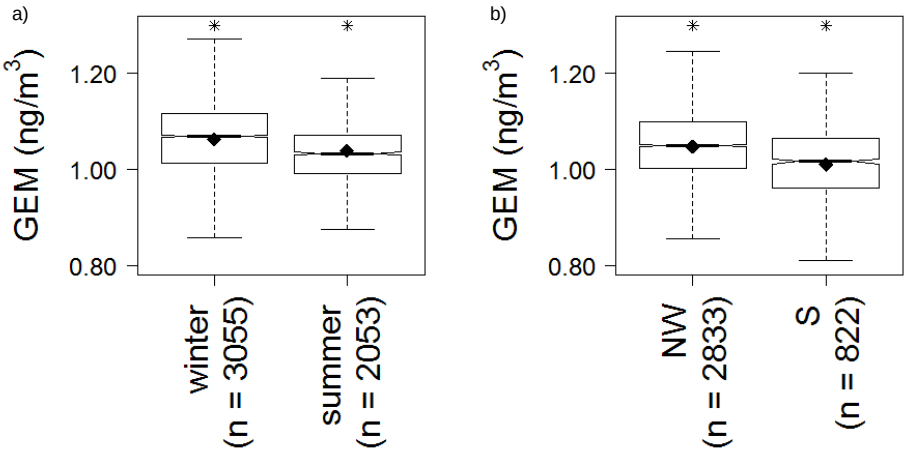

Figure 4. Hourly-average gaseous elemental mercury (GEM) concentrations (ng m^{-3}) measured at Amsterdam Island: **(a)** in winter (July–September) or summer (December–February), and **(b)** under northwesterly (NW) or southerly (S) winds. ♦: mean, ∗: statistically significant difference, n = number of hourly-average data, bottom and top of the box: first and third quartiles, band inside the box: median, ends of the whiskers: lowest (highest) datum still within 1.5 interquartile range of the lower (upper) quartile. Outliers are not represented.

ACPD
14, 14439–14470, 2014

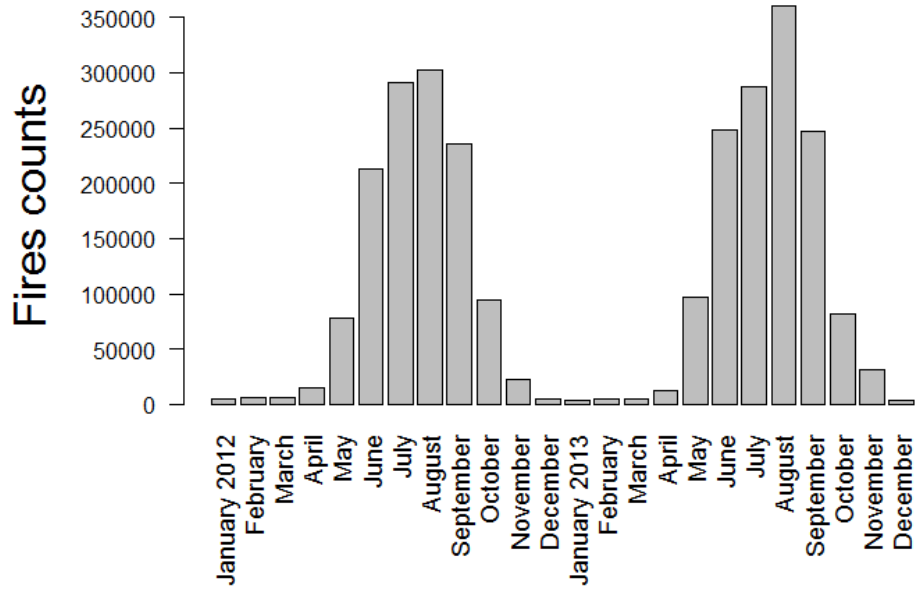

Figure 5. Fires counts west of Amsterdam Island (latitude: 3–53° S, longitude: 10–73° E) in 2012 and 2013. Data courtesy of FIRMS MODIS Fire Archive Download.

ACPD
14, 14439–14470, 2014

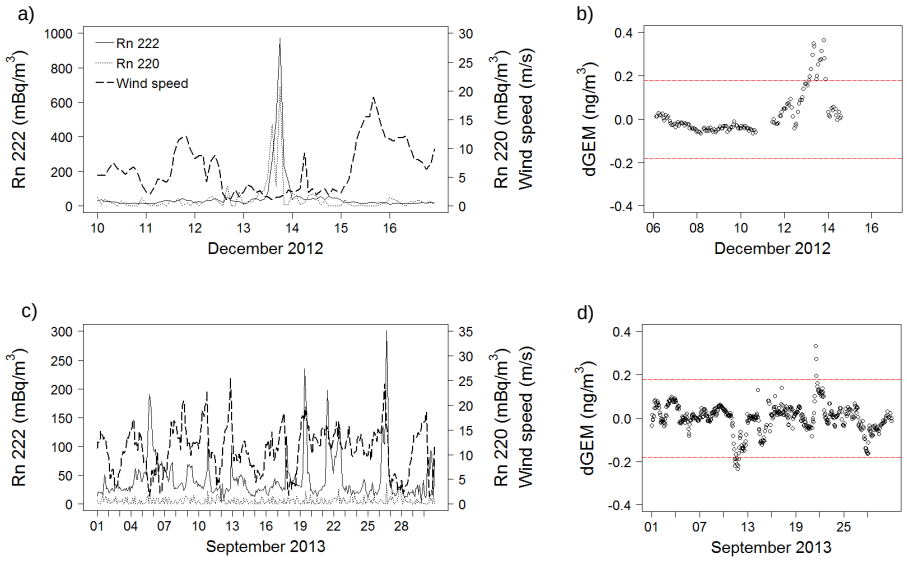

Figure 6. Examples of ^{222}Rn (mBq m^{-3}) peaks observed at Amsterdam Island along with ^{220}Rn (mBq m^{-3}) activity and wind speed (m s^{-1}): **(a)** in December 2012, **(c)** in September 2013. Background variability (dGEM, ng m^{-3}) of GEM concentrations observed at Amsterdam Island in: **(b)** December 2012, **(d)** September 2013. Dotted lines represent 3 times the mean monthly standard deviation of dGEM measurements.

ACPD
14, 14439–14470, 2014

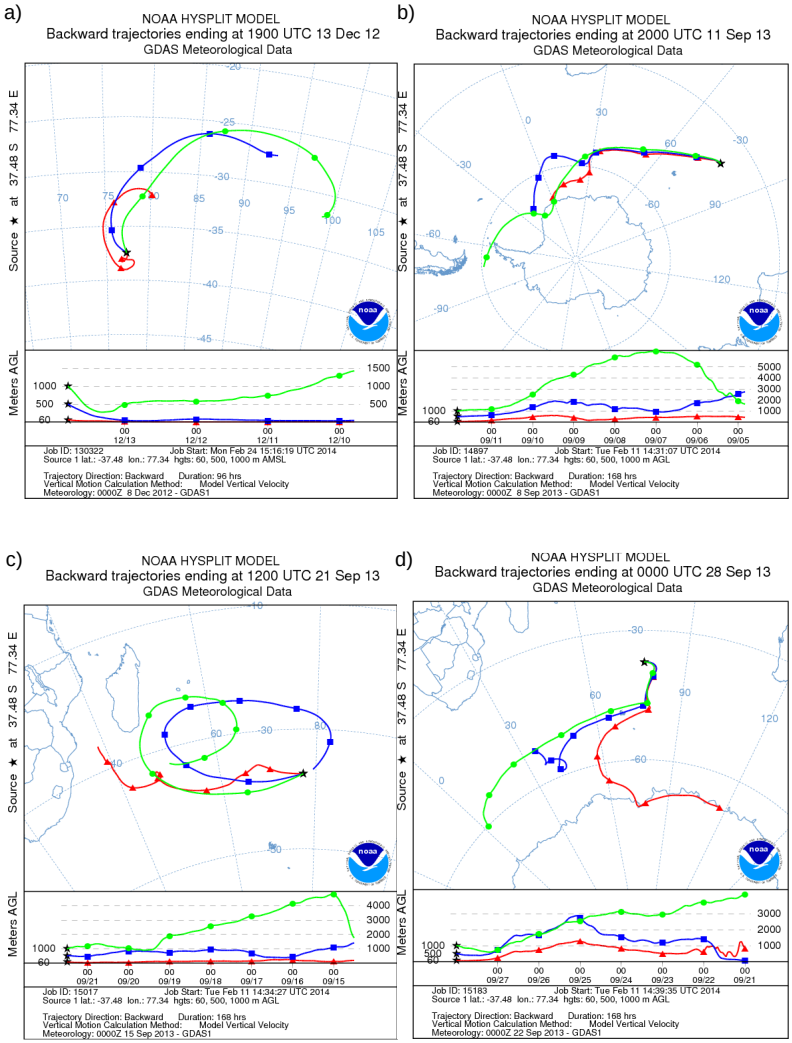

ACPD
14, 14439–14470, 2014

A 2 year record of atmospheric Hg at a background Southern Hemisphere station

H. Angot et al.

Figure 7. Back trajectories ending on Amsterdam Island (★) on **(a)** 13 December 2012, **(b)** 11 September 2013, **(c)** 21 September 2013 and **(d)** 28 September 2013. Data courtesy of NOAA.

ACPD
14, 14439–14470, 2014

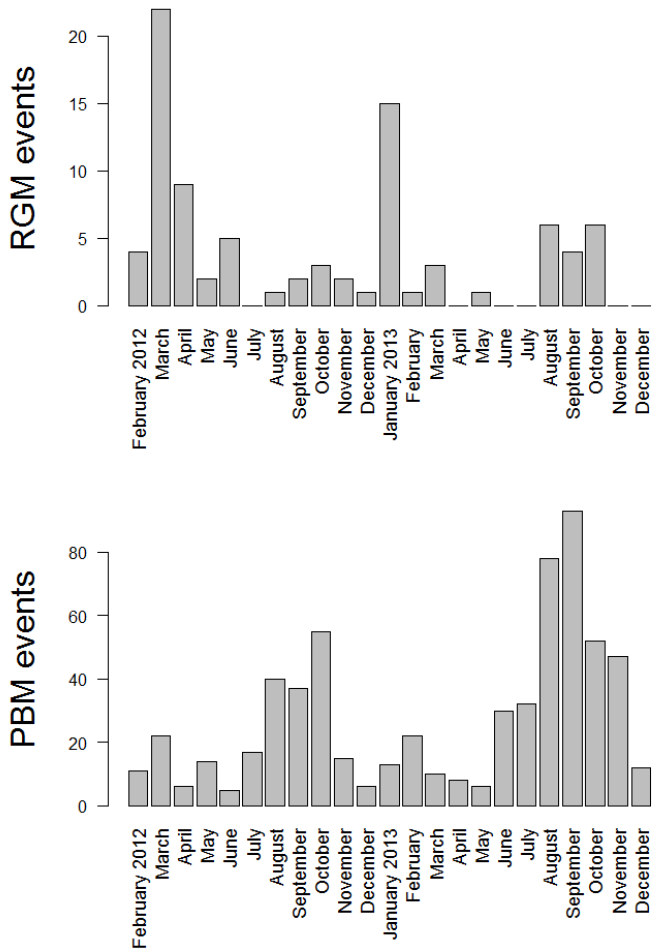

Figure 8. Reactive gaseous mercury (RGM) and particle-bound mercury (PBM) events at Amsterdam Island from February 2012 to December 2013.

ACPD
14, 14439–14470, 2014

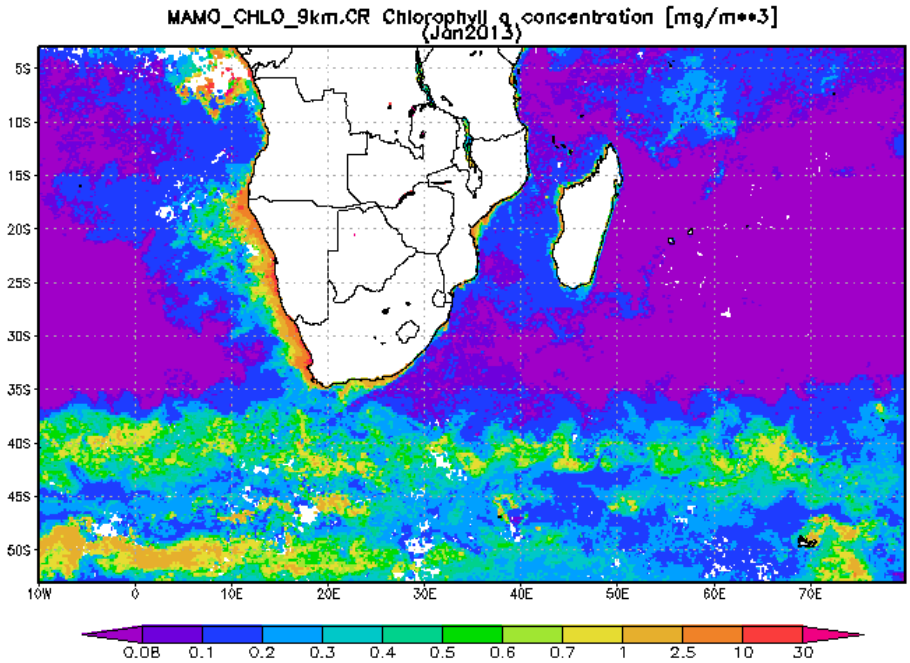

Figure 9. SeaWIFS chlorophyll *a* map (January 2013) of the Indian sector of the Austral Ocean. Data courtesy of Giovanni online data system.

ACPD
14, 14439–14470, 2014

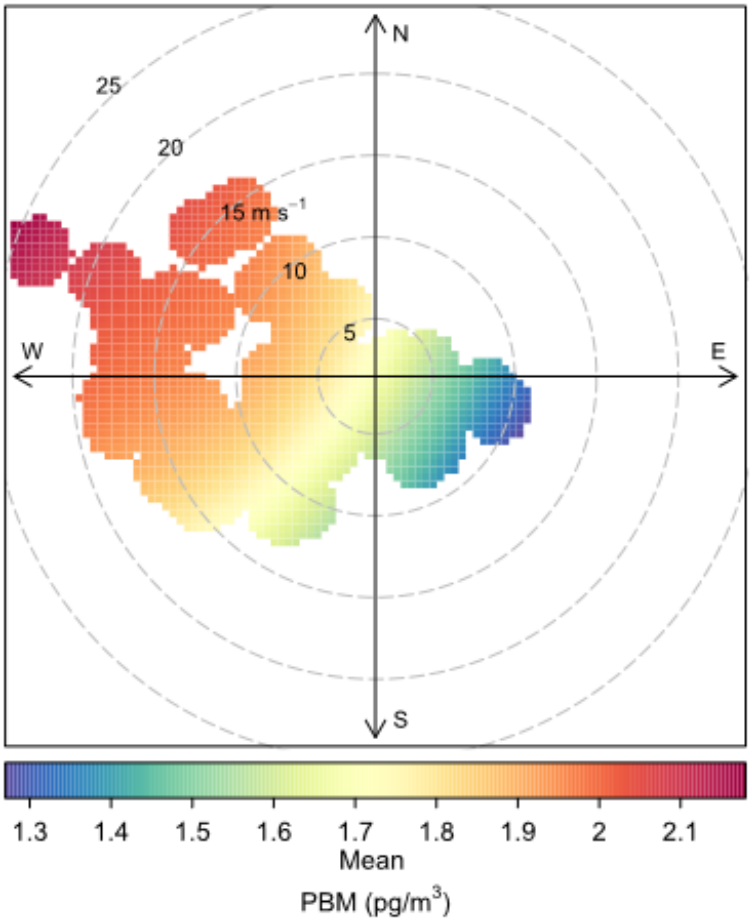

Figure 10. Particle-bound mercury (PBM) concentrations (pg m^{-3}) according to wind speed (m s^{-1}) and direction. N: North, E: East, S: South, W: West.

ACPD
14, 14439–14470, 2014